International Journal of Heat and Mass Transfer 51 (2008) 6054–6062

Contents lists available at ScienceDirect

International Journal of Heat and Mass Transfer

journal homepage: www.elsevier.com/locate/ijhmt

Conjugate heat transfer by natural convection, conduction and radiation in open cavities

H. Nouanegue, A. Muftuoglu, E. Bilgen *

Ecole Polytechnique Box 6079, centre ville, Montreal, QC, Canada H3C 3A7

ARTICLE INFO

Article history:
Received 15 September 2007
Received in revised form 16 May 2008
Available online 2 July 2008

Keywords:
Conjugate heat transfer
Natural convection
Conduction
Radiation
Open cavity

ABSTRACT

In this paper, we investigate conjugate heat transfer by natural convection, conduction and radiation in open cavities in which a uniform heat flux is applied to the inside surface of the solid wall facing the opening. Conservation equations are solved by finite difference–control volume numerical method. The relevant governing parameters are: the Rayleigh numbers from 10^9 to 10^{12}, the Prandtl number, $Pr = 0.7$, constant for air, the cavity aspect ratio, $A = L/H$ from 0.4 to 1, the wall thickness $l/H = 0.02$–0.08, the conductivity ratio k_r from 1 to 50 and the surface emissivity, ε from 0 to 1. We found that the surface radiation affected the flow and temperature fields considerably. The influence of the surface radiation is to decrease the heat fluxes by natural convection and conduction while the heat flux by radiation increases with increasing surface emissivity. On the other hand, the convective and radiative Nusselt numbers are increasing functions of the surface emissivity for a given wall conductance. The combined Nusselt number and the volume flow rate are both increasing functions of the surface emissivity, particularly at high Rayleigh numbers. The convective and radiative Nusselt numbers are a decreasing function of the wall conductance and an increasing function of the aspect ratio. We found similar trends for the volume flow rate through the cavity.

1. Introduction

Open cavities are encountered in various engineering systems, such as open cavity solar thermal receivers, uncovered flat plate solar collectors having rows of vertical strips, electronic chips, passive systems, etc. For example, in applications such as flat plate solar collectors, two or three dimensional small open cavities are used to reduce thermal losses. In these applications, the order of magnitude of cavity dimensions is usually small; hence, the heat transfer is usually by laminar natural convection. However, the heat flux may create such a high temperature that the resulting radiation heat exchange would be significant. Indeed, experimental studies show that this is the case (e.g. [1,2]). The situation is certainly similar in open cavity solar receivers and electronic cooling cases where the heat flux may be high. A literature review shows that there are numerous studies on heat transfer by natural convection in open cavities, numerical (e.g. [3–10]) as well as experimental (e.g. [11–14]), and by conjugate heat transfer (e.g. [15–20]).

Representative numerical studies may be categorized as: (i) side facing horizontal and inclined open cavities with an aspect ratio of one (e.g. [3–6]), (ii) horizontal and inclined shallow cavities with isothermal or constant heat flux at the side facing the opening (e.g. [7,8]), (iii) similar to the cases (i) and (ii) above but open cavities having solid walls (e.g. [9]). In the first two cases, heat transfer by natural convection only is considered, i.e. conduction and radiation are neglected; in the last case, heat transfer by natural convection and conduction is considered but radiation is neglected. Similarly, experimental studies have been performed using open cavities with an aspect ratio of one (e.g.[11–13]), in shallow cavities [1,14] and in inclined cavities where radiation heat exchange is not negligible [2].

Theoretical conjugate heat transfer by natural convection and radiation has been studied in various other geometries. Indirectly related to our study, those in enclosures (e.g. [15,16]) and in open cavities with side and top openings (e.g. [17,18]) may be mentioned. Akiyama and Chong [15] studied conjugate heat transfer by natural convection and radiation in a square cavity. Ramesh and Venkateshan [16] studied the effect of surface radiation on heat transfer by natural convection in a square cavity. Ramesh and Merzkirch [17] studied experimentally conjugate heat transfer by convection and radiation in side vented open cavities with top opening. They found that for cavities with low emissive walls natural convection was the dominant mode; with high emissive walls, both natural convection and radiation were competitive modes contributing equally to the total heat transfer. Singh and Venkateshan studied numerically the same problem [18]. They found that

* Corresponding author. Tel.: +1 514 340 4711x4579; fax: +1 514 340 5917.
E-mail address: bilgen@polymtl.ca (E. Bilgen).

0017-9310/$ - see front matter © 2008 Elsevier Ltd. All rights reserved.
doi:10.1016/j.ijheatmasstransfer.2008.05.009

Nomenclature

A	enclosure aspect ratio, = L/H
c_p	heat capacity, J/kg K
F_{ij}	configuration factor
g	acceleration due to gravity, m/s^2
H	cavity height, m
k	thermal conductivity, W/m K
k_r	conductivity ratio, k_s/k_f
L	cavity width, m
l	wall thickness, m
N_r	radiation number,= $\sigma T_\infty^4/q''$
Nu	Nusselt Number
Nu_r	Radiative Nusselt number, = $h_r H/k_f$
p	pressure, Pa
P	dimensionless pressure, = $(p-p_\infty)H^2/\rho\alpha^2$
Pr	Prandtl number, = υ/α
q''	heat flux, W/m^2
q	dimensionless heat flux, = $\frac{\partial\theta}{\partial X}$
Ra	Rayleigh number, = $g\beta q''H^4/(\upsilon\alpha k)$
t	time, s
U, V	dimensionless fluid velocities, = uH/α, vH/α
$\dot{V}$	dimensionless volume flow rate through the opening
X,Y	dimensionless Cartesian coordinates, = x/H, y/H,
x, y	Cartesian coordinates

Greek symbols

α	thermal diffusivity, m^2/s
α_r	thermal diffusivity ratio,= α_s/α_f
β	volumetric coefficient of thermal expansion, 1/K
Γ	general diffusion coefficient
δ_{ij}	Kronecker delta
ε	surface emissivity
ζ	dimensionless radiative heat flux,= $q_r/\sigma T_\infty^4$
Θ	temperature ratio,= T/T_∞
θ	dimensionless temperature, = $(T-T_\infty)/(Hq''/k)$
υ	kinematic viscosity, m^2/s
ρ	fluid density, kg/m^3
σ	Stefan–Boltzmann constant
τ	dimensionless time, = $\alpha t/H^2$
ψ	stream function

Subscripts

c	convection
cn	conduction
ext	extremum
f	fluid
in	into cavity
max	maximum
opt	optimum
out	out of the cavity
r	radiation, ratio
s	solid
t	total or combined
∞	ambient value
1	at the wall surface, X = l/H
2	at the exit plane, $X = A$

radiation changed the flow pattern and the thermal performance in side vented cavities with top opening. Studies of conjugate heat transfer involving surface radiation in open cavities were reported in [19,20]. Dehghan and Behnia [19] studied numerically conjugate heat transfer by three modes in an open-top upright cavity having discrete heater and with the bottom side insulated. They have also done some experimental observations regarding flow patterns. They found that the surface radiation had a significant effect on the flow but a negligible one on the heat transfer performance; there was also good agreement with their experimental study. Hinojosa et al. [20] studied numerically conjugate heat transfer by natural convection and radiation in an inclined cavity with isothermal wall facing the opening and insulated other two boundaries. They found that the convective Nusselt number increased with the inclination angle while the radiative Nusselt number stayed quasi-constant.

In the present study, we address the case of conjugate heat transfer by natural convection, conduction and radiation in open cavities with a heated solid wall facing the opening and the other two boundaries, perpendicular to the end wall, insulated. We determine the influence of the surface radiation on the other modes of heat transfer and the importance of each as a function of the governing parameters.

2. Problem and mathematical model

Schematic of the two dimensional open cavity with a uniform heat flux on the inner surface of the wall and the boundary conditions are shown in Fig. 1. Horizontal boundaries of the cavity are adiabatic, the left face of the solid wall is isothermal and its right side is in the open cavity, which is in contact with the ambient air. The inner side of the wall is heated at constant heat flux, q''.

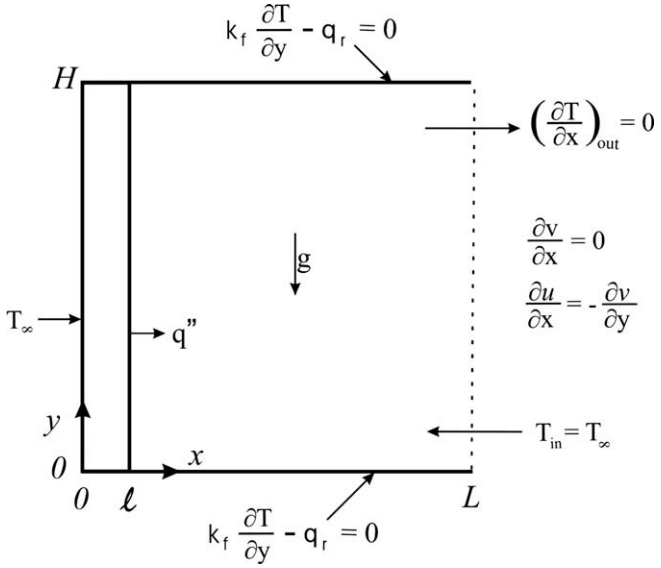

Fig. 1. Schematic of open cavities, the coordinate system and boundary conditions.

2.1. Convection and conduction formulation

We assume that the fluid is Newtonian, and the third dimension has a negligible effect on the flow and heat transfer. With these assumptions, we use two dimensional conservation equations for mass, momentum and energy with Boussinesq approximation. By using H as the length scale, α/H as the velocity scale, Hq''/k as the temperature scale, $\rho\alpha^2/H^2$ as the pressure scale and H^2/α as the time scale, we obtain following non-dimensional equations

$$\frac{\partial U}{\partial X}+\frac{\partial V}{\partial Y}=0 \tag{1}$$

$$\frac{\partial U}{\partial \tau}+U\frac{\partial U}{\partial X}+V\frac{\partial U}{\partial Y}=-\frac{\partial P}{\partial X}+\Gamma Pr\nabla^2 U \tag{2}$$

$$\frac{\partial V}{\partial \tau}+U\frac{\partial V}{\partial X}+V\frac{\partial V}{\partial Y}=-\frac{\partial P}{\partial Y}+\Gamma Pr\nabla^2 V+RaPr\theta \tag{3}$$

$$\frac{\partial \theta}{\partial \tau}+U\frac{\partial \theta}{\partial X}+V\frac{\partial \theta}{\partial Y}=\alpha_r\nabla^2\theta \tag{4}$$

We note that we are using unsteady state equations to obtain steady state solutions. Γ in Eqs. (2) and (3) is a general diffusion coefficient, which is equal to 1 in the fluid region and 10^{15} in the solid region; it is introduced to ensure that $U = V = 0$ everywhere including at the solid–fluid interface. α_r in Eq. (4) is the ratio of the thermal diffusivities α_s/α_f and it is equal to 1 in the fluid region and α_s/α_f in the solid region. In numerical simulation at each time step, we have to satisfy the energy conservation at the interface between the solid and the fluid, i.e. in the X direction for example, $k_r\partial\theta_s/\partial X = \partial\theta_f/\partial X$ with $k_r = k_s/k_f$. For the steady state solution with $\partial\theta/\partial\tau = 0$ and $\alpha_r = k_r$, we have Eq. (4) in its simplified form.

2.2. Radiation formulation

We assume that the walls are diffuse and grey, and the air is a non-absorbing medium. For an area on a surface the non-dimensional energy conservation equation is obtained by introducing $\Theta = T/T_\infty$ and $\zeta_i = q_i/\sigma T_\infty^4$ in the dimensional equation in [21]

$$\sum_{j=1}^{n}(\delta_{ij}-F_{ij})\Theta_j^4=\sum_{j=1}^{n}[\delta_{ij}-(1-\varepsilon_j)F_{ij}]\frac{\zeta_j}{\varepsilon_j} \tag{5}$$

where F_{ij} is the configuration factor and n is the number of surface areas.

At the surface:

$$N_r\zeta=\left(\frac{\partial\theta_f}{\partial X}-k_r\frac{\partial\theta_s}{\partial X}\right) \tag{6}$$

where $N_r=\frac{\sigma T_\infty^4}{q''}$ is the radiation number, $\frac{\partial\theta_f}{\partial X}$ and $\frac{\partial\theta_s}{\partial X}$ are the heat fluxes from the wall surface to the fluid and from the same surface to the solid wall, respectively.

The governing parameters are $Ra = g\beta q'' H^4/(\upsilon\alpha k)$, $Pr = \upsilon/\alpha$, k_r, ε, and $A = L/H$ and l/H.

The average convective Nusselt number is calculated at the inner wall surface $X = l/H$ as

$$Nu_c=\frac{-\int_0^1\frac{\partial\theta}{\partial X}dY}{\int_0^1(\theta_1-\theta_2)dY} \tag{7}$$

The average radiative Nusselt number is calculated at $X = l/H$ as

$$Nu_r=\frac{\int_0^1 N_r\zeta_s dY}{\int_0^1(\theta_1-\theta_2)dY} \tag{8}$$

The volume flow rate, $\dot{V}$ is calculated as

$$\dot{V}=-\int_{X=A}U_{in}dX \tag{9}$$

where $U_{in} = U_{X=A}$ if $U_{X=A} < 0$ and $U_{in} = 0$ if $U_{X=A} \geqslant 0$

The stream function is calculated from its definition as

$$U=-\frac{\partial\psi}{\partial Y},\quad V=\frac{\partial\psi}{\partial X} \tag{10}$$

ψ is zero on the solid surfaces and the streamlines are drawn by $\Delta\psi = (\psi_{max}-\psi_{min})/n$ with n is the number of increments. Boundary conditions are

$$\text{On solid surfaces}: U=0, V=0 \tag{11}$$

$$X=0 \quad \text{to} \quad l/H, Y=0 \quad \text{and} \quad 1: \quad \frac{\partial\theta}{\partial n}=0 \tag{12a}$$

$$X=l/H \quad \text{to} \quad A, \quad Y=0 \quad \text{and} \quad 1 \quad -\frac{\partial\theta}{\partial n}+N_r\varsigma=0 \tag{12b}$$

$$X=0, \quad Y=0 \quad \text{to} \quad 1: \quad \theta=0 \tag{13}$$

$$X=A, \quad Y=0 \quad \text{to} \quad 1: \quad \frac{\partial V}{\partial X}=0, \quad \frac{\partial U}{\partial X}=-\frac{\partial V}{\partial Y},$$

$$\theta_{in}=0, \quad \left(\frac{\partial\theta}{\partial X}\right)_{out}=0 \tag{14}$$

The boundary condition at the opening, Eq. (14) is shown to be satisfactory for the case of confined computation domain in the open cavity with respect to that extended computation domain [9]. The boundary condition for the temperature is such that for the fluid entering the cavity it is $\theta_{in} = 0$ and for the outgoing fluid $(\partial\theta/\partial X)_{out} = 0$. The heater on the inside surface of the wall has a heat flux of $q = 1$.

3. Numerical technique

The numerical method used to solve Eqs. (1)–(6) with the boundary conditions Eqs. (11) – (14) is the SIMPLER (semi-implicit method for pressure linked equations revised) algorithm [22]. The computer code based on the mathematical formulation presented above and the SIMPLER method were validated with the benchmark [23]. The results showed that the deviations in Nusselt number and the maximum stream function at $Ra = 10^5$ were 1.84% and 0.97%, respectively. Similarly at $Ra = 10^6$, they were 1.74% and 1.09%, respectively. It was seen that the concordance was excellent. In addition, the average Nusselt numbers at the hot and cold walls of the benchmark problem were compared, which showed a maximum difference of about 0.5% in all runs. The present code was tested also to simulate the case of conjugate heat transfer by conduction and convection in open cavities [9]. The results are presented in Table 1, which shows an excellent agreement. Additionally, we simulated the case of conjugate heat transfer by convection and radiation in a square cavity [15]. The results presented in Table 2 show good agreements.

Uniform grid in X and Y direction was used for all computations. Grid convergence was studied for the case of square cavity having $l/H = 0.05$ and $k_r = 20$ with grid sizes from 31×21 to 71×61 at $Ra = 10^{11}$. The results are presented in Table 3. We see that 41×31 and 51×41, the variation in Nusselt is 1.19%, it is 0.59% in volume flow rate, and 0.73% in radiative heat flux. Thus, 41×31 grid size was a good choice from the computation time and precision point of view for the square cavity. We conducted similar tests with the shallow and tall cavities and used 41×31 for $A = 0.7$ and 41×31 for $A = 0.4$ grid sizes. The grid size in the wall was 2, 5 and 8 in the X direction for the wall thickness of $l/H = 0.02$, 0.05 and 0.08, respectively, and the rest were in the cavity. Using a computer with a dual processor of 1.83 GHz clock speed, for $A = 1$, with 41×31 grid size, at $Ra = 10^{10}$, the typical execution time was 234 s and at $Ra = 10^{11}$, it was 284 s.

A converged steady state solution was obtained by iterating in time until variations in the primitive variables between subsequent time steps were:

$$\sum|(\phi_{i,j}^{old}-\phi_{i,j})|<10^{-4} \tag{15}$$

where ϕ stands for U, V, and θ.

Table 1
Validation study of natural convection and conduction in an open square cavity [9]

Ra	$Nu/\dot{V}$ [9]	$Nu/\dot{V}$[This study]	% Deviations
10^6	1.01/0.20	1.016/0.190	−0.00594/0.05000
10^8	2.75/6.13	2.870/6.144	−0.04364/−0.00223
10^{10}	11.32/35.52	12.012/33.216	−0.06111/−0.02139
10^{12}	40.01/122.00	38.100/125.434	0.04774/−0.02815

Table 2
Validation study of natural convection and radiation in a square enclosure [15]

Θ_0	ΔT, K	d, m	ε	This study			[15]			% Deviations
				Nu_c	Nu_r	Nu_t	Nu_c	Nu_r	Nu_t	
41.7	10	0.264	1.0	4.013	11.254	15.267	3.861	11.220	15.281	3.94/0.30/1.23
41.7	10	0.264	0.0	4.175	0	4.175	4.150	0	4.150	0.60/0/0
1.6	260	0.0891	1.0	3.301	4.411	7.712	3.471	4.481	7.952	4.89/1.57/3.02
1.6	260	0.0891	0.0	4.175	0	4.175	4.146	0	4.146	0.70/0/0.70

Table 3
Grid independence study at $Ra = 10^{10}$ with $A = 1$, $l/H = 0.05$, $k_r = 20$

Size	Nu_c	%	Nu_r	%	$\dot{V}$	%	q_r/q_t	%
31×21	8.731	*3.87*	20.217	*4.51*	29.216	*2.71*	0.00200	*2.82*
41×31	8.888	*2.14*	19.815	*2.43*	28.672	*0.80*	0.00203	*1.60*
51×41	8.996	*0.95*	19.576	*1.19*	28.502	*0.20*	0.00204	*0.87*
61×51	9.045	*0.41*	19.397	*0.27*	28.482	*0.13*	0.00205	*0.49*
71×61	9.082	*0.00*	19.345	*0.00*	28.445	*0.00*	0.00206	*0.00*

Within the same time step, the residual of the pressure term was less than 10^{-3} [22]. In addition, the accuracy of the solution was double-checked using the energy conservation on the domain to ensure it was less than 10^{-4}.

4. Results and discussion

The variable geometrical parameters considered are, the aspect ratio, $A = 0.4$, 0.7 and 1, and the dimensionless wall thickness, $l/H = 0.02$, 0.05 and 0.08. The Rayleigh number was varied from $Ra = 10^9$ to 10^{12}. The Prandtl number, $Pr = 0.70$ for air was kept constant. The conductivity ratio was varied from $k_r = 1$ to 50, the first one is for insulation materials and the second for common industrial materials. We will present first the results for the aspect ratio, $A = 1$ and then the effect of it on the results. We will be using the Rayleigh number, $Ra = g\beta q'' H^4/k\alpha\nu$ to present both Nu_c and Nu_r defined in the nomenclature as well as the total Nusselt number, Nu_t. For the simulation of the system shown in Fig. 1, we specified $H = 0.727$ m, $T_\infty = 300$ K. We had the following range for the radiation number: $459 < N_r < 0.459$ at Ra from 10^9 to 10^{12}, respectively; i.e. N_r is a decreasing function of Ra.

4.1. Flow patterns and isotherms

We will examine the effect of radiation on the flow and temperature fields for the case of $A = 1$, $l/H = 0.05$, $k_r = 20$, $\varepsilon = 0$, 0.5, 1 and at $Ra = 10^{10}$, 10^{11} and 10^{12}. We present the streamlines in Fig. 2 and the isotherms in Fig. 3. The flow patterns at three Rayleigh numbers in Fig. 2 for the case without radiation, i.e. $\varepsilon = 0$, are shown in the first column. We see that the air enters the cavity from the lower part of the opening, rises along the heated wall and following upper horizontal boundary it exits at the upper part of the opening. As expected, the flow pattern changes as the Rayleigh number is increased from 10^{10} to 10^{11} and then 10^{12}. Indeed, Ψ_{ext} is increased from -27.2628 at $Ra = 10^{10}$ to -55.6181 at 10^{11} and then to -107.7358 at 10^{12}. For $\varepsilon = 0.5$ in the second column of Fig. 2, we see that the flow pattern has changed with respect to that with $\varepsilon = 0$ in the first column of Fig. 2, particularly as the Rayleigh number is increased from 10^{10} to 10^{12}. The strength of the air circulation through the cavity is increased: Ψ_{ext} is -28.2983 at $Ra = 10^{10}$, it is increased to -56.4030 at 10^{11} and then to -127.9201 at 10^{12}. We see that Ψ_{ext} is increased with respect to those with $\varepsilon = 0$. For $\varepsilon = 1$, i.e. black body radiation shown in the third column of Fig. 2, the change in the flow pattern is further enhanced but its appearance is almost the same as for $\varepsilon = 0.5$ case at $Ra = 10^{10}$ and 10^{11}. The change is more striking at $Ra = 10^{12}$, as the cavity air becomes more stratified. Ψ_{ext} is -29.8091 at $Ra = 10^{10}$, it is increased to -57.2141 at 10^{11} and then to -136.9932 at 10^{12}.

The isotherms corresponding to the same cases of Fig. 2 are shown in Fig. 3. We see that the influence of the surface radiation on the temperature field is visibly important. The temperature gradient for $\varepsilon = 0$ is mainly confined at the heated wall. Yet with the surface radiation in Fig. 3b and c, the temperature gradients on the heated wall as well as on the adiabatic horizontal boundaries are important. The isotherms near the corners are bent towards the corners, thus indicating higher temperature gradients. We see also that the isotherms in the solid wall show higher temperature gradients with surface radiation, hence important heat transfer by conduction.

The flow and temperature fields for $A = 0.7$ and 0.4, $l/H = 0.05$, $k_r = 20$, $\varepsilon = 0$ and 1 and at $Ra = 10^{11}$ are shown in Fig. 4. We see that the flow and temperature fields are modified by the surface radiation in a manner similar to the case with $A = 1$. For $A = 0.7$, $\varepsilon = 0$ and $\varepsilon = 1$, Ψ_{ext} is -53.6804 and -55.8196, respectively; for $A = 0.4$, $\varepsilon = 0$ and $\varepsilon = 1$ it is -51.2875 and -53.3797, respectively, i.e. the strength of convection is increased with the surface radiation. Again, the temperature gradients on the adiabatic horizontal boundaries are strikingly different from the case with no-surface radiation. Thus, we expect that the heat transfer will accordingly be affected by the surface radiation exchange in tall open cavities.

The influence of surface radiation on the velocity, U and the temperature, θ at the exit plane, $X = A$ is presented in Fig. 5a and the local convection Nusselt number, Nu_{loc} at the planes of $X = 0.05\ A$, $0.6\ A$ and $X = A$ is presented in Fig. 5b for the case of $A = 1$, $l/H = 0.05$, $k_r = 20$ with $Ra = 10^{10}$. We see in Fig. 5a that the profiles of variations of U and θ follow the description of the flow and temperature fields in Figs. 2 and 3. For $\varepsilon = 1$, the velocity profile of the cold fluid entering the cavity becomes more uniform. The temperature profile at the entrance is modified along the bottom wall as well as along the upper wall. In addition, we see important modifications near the corners, due to higher temperature gradients as observed with Fig. 3. Thus, the influence of surface radiation is to change the temperatures on the enclosure walls, including the adiabatic ones. For the same case, the influence of surface radiation on the convective local Nusselt number in Fig. 5b is to modify it along the bottom and upper adiabatic walls as seen at all three planes, and make more uniform along the heated vertical wall as seen at $X = 0.05\ A$ plane. Thus, the variation of the local Nusselt number is modified for $\varepsilon = 1$ in such a way to have a high convective local Nusselt number at the bottom and top, and reduced values in between than those for $\varepsilon = 0$. These representative results confirm indeed our observations of the flow and temperature fields discussed earlier with Figs. 2 and 3.

4.2. Heat transfer and volume flow rate

In conjugate heat transfer by conduction, convection and radiation, the total heat flux, $q_t = q''$ is the sum of the heat fluxes, q_{cn}, q_c, q_r, respectively. Hence

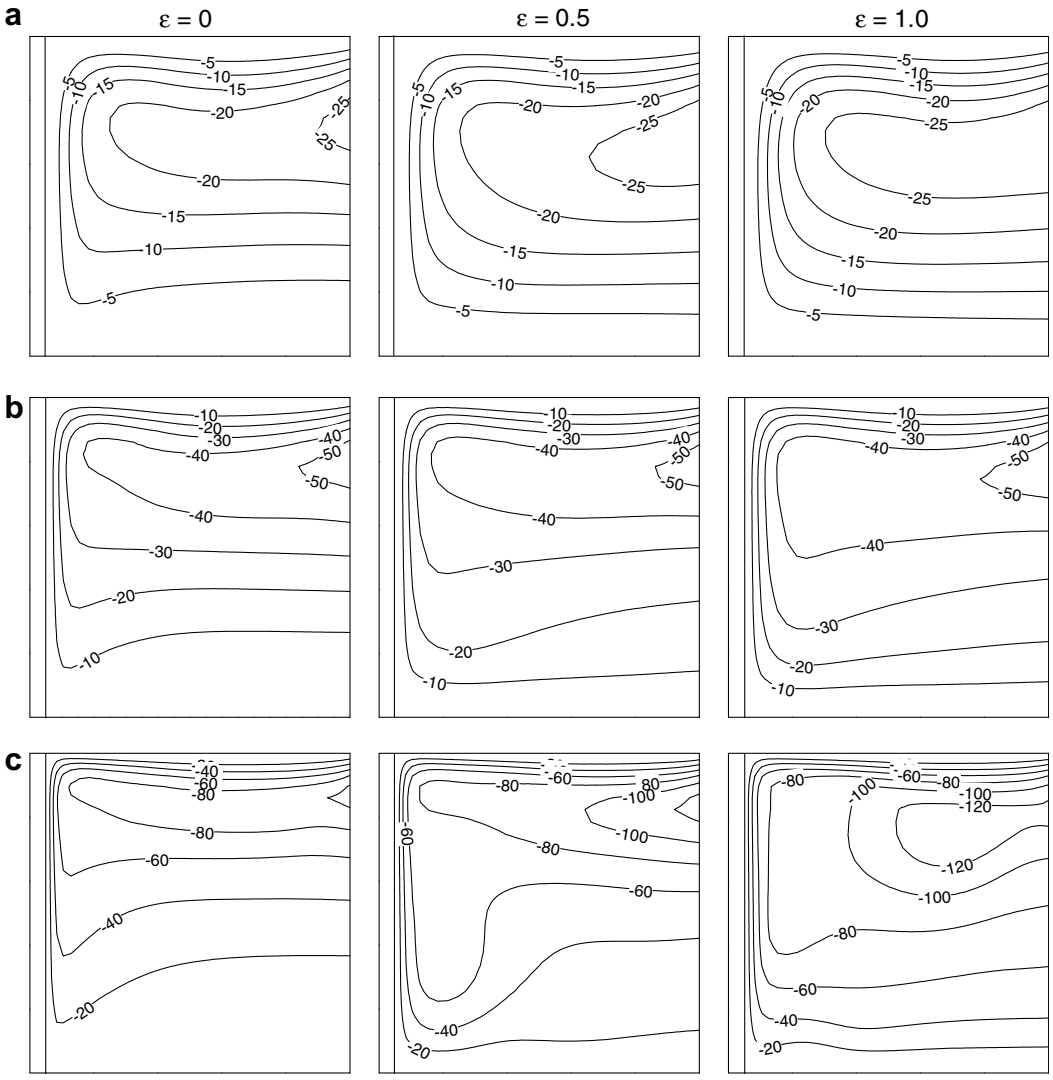

Fig. 2. Streamlines for $A = 1$, $l/H = 0.05$, $k_r = 20$ and $\varepsilon = 0$, 0.5 and 1.0 and (a) $Ra = 10^{10}$, (b) $Ra = 10^{11}$ and (c) $Ra = 10^{12}$.

$$\frac{q_{cn}}{q_t} + \frac{q_c}{q_t} + \frac{q_r}{q_t} = 1 \tag{16}$$

For the case with $A = 1$, $l/H = 0.05$ and $\varepsilon = 1$ with k_r as a parameter, we present q_i/q_t (i takes c, cn and r) as a function of the Rayleigh number in Fig. 6. We observe that as expected, the heat flux by conduction, q_{cn} is slightly decreasing with Ra and it is increasing with k_r, which is expected because the wall surface temperature θ_1 slightly decreases with Ra. The heat flux by natural convection, q_c is an increasing function of Ra and a decreasing function of k_r, which is expected. As a result and following Eq. (16), the heat flux by radiation, q_r is slightly decreasing function of the Rayleigh number, Ra and a decreasing function of the conductivity ratio, k_r. In particular, we note that the heat flux by natural convection decreases when the conductance through the wall increases. For $k_r = 1$, a quasi-insulated wall, the conductance is small, the natural convection has the same order of magnitude as the conduction. Obviously, the heat flux by natural convection increases with the Rayleigh number, as a result of which the heat flux by radiation decreases accordingly. We note also that the order of magnitudes of the heat flux by radiation is the highest in this case. For example, at $Ra = 10^{12}$, the heat flux is 0.16 by conduction, 0.62 by radiation and 0.22 by natural convection. For $k_r = 20$, the conductance is high and the order of magnitude of heat fluxes by convection and radiation is low. For example, at $Ra = 10^{12}$, the heat flux is 0.75 by conduction, 0.18 by radiation and 0.07 by natural convection. This trend is further magnified for $k_r = 50$ (not shown here) and the percentages become as 0.89, 0.08 and 0.03, respectively. We see that the influence of the surface radiation on natural convection is important at any wall conductance case.

To see the influence of surface radiation on heat fluxes by conduction and convection, the data of q_i/q_t versus ε are plotted in Fig. 7 with Ra as parameter. We see that both heat fluxes by conduction and natural convection, q_{cn}/q_t and q_c/q_t, are a decreasing function of ε, and the heat flux by radiation is an increasing function of it. Thus, as expected the influence of surface radiation on the conductive and convective heat fluxes is to decrease them as the surface emissivity is increased from 0 to 1.

The average Nusselt numbers by Eqs. (7), and (8) and the volume flow rate $\dot{V}$ by Eq. (9) are calculated as a function of the Rayleigh number and presented in Fig. 8 for the same case of $A = 1$ with l/H, $\varepsilon = 1$ and k_r as parameters. Following the results of Fig. 6, the Nusselt number by natural convection, Nu_c is an increasing function of the Rayleigh number, Ra and decreasing function of the conductivity ratio, k_r. The radiative Nusselt number, Nu_r is quasi-constant at high Rayleigh numbers but dependent on k_r at low Ra numbers. The contribution by each mode of heat transfer is

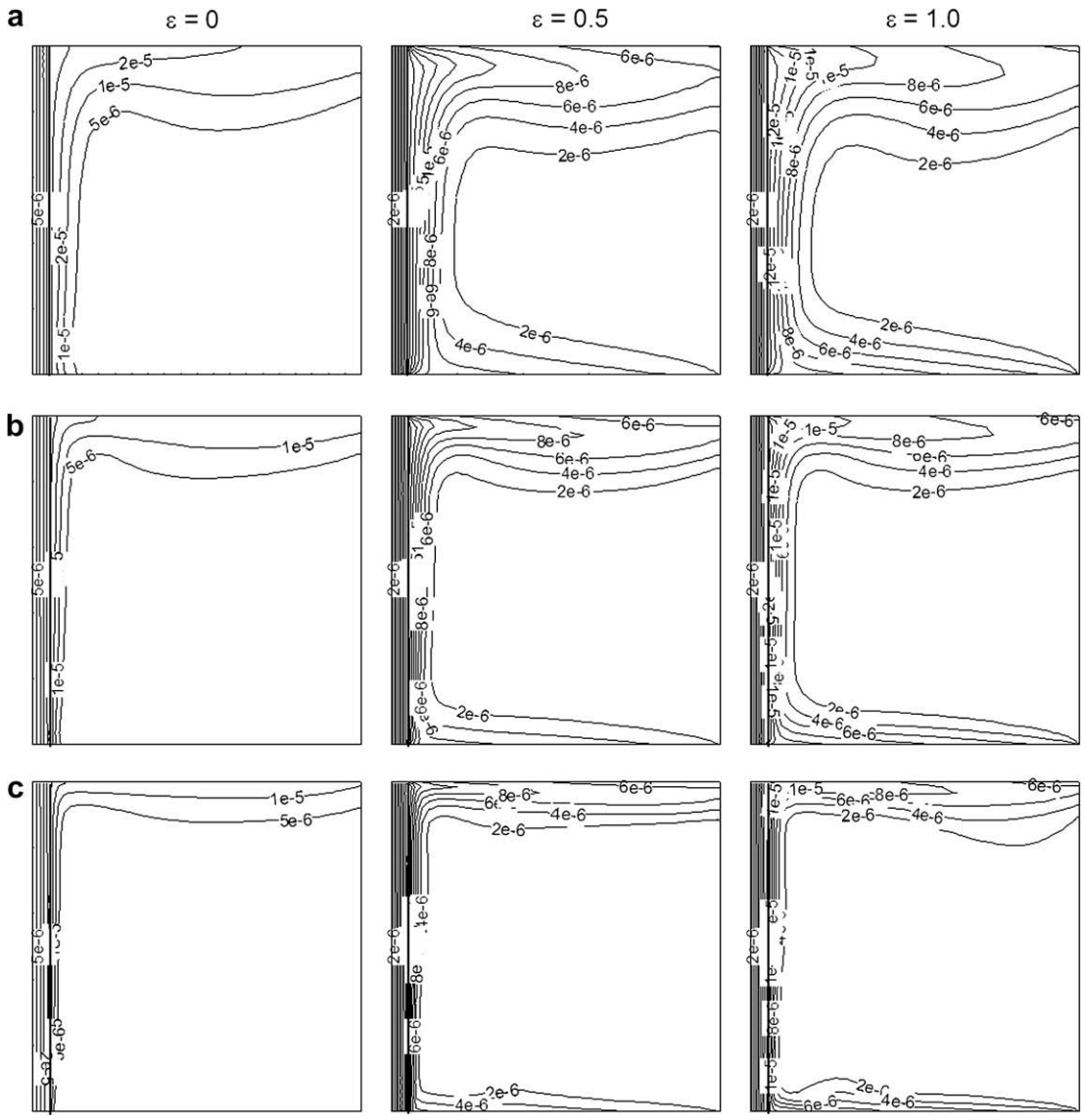

Fig. 3. Isotherms corresponding to Fig. 2 for $A = 1$, $l/H = 0.05$, $k_r = 20$ and $\varepsilon = 0$, 0.5 and 1.0 and (a) $Ra = 10^{10}$, (b) $Ra = 10^{11}$ and (c) $Ra = 10^{12}$.

Rayleigh number dependent; at high Rayleigh numbers; for example at $Ra = 10^{12}$, Nu_c is from 24 to 34 for $k_r = 1$ to 50, while Nu_r is about 20 although it is slightly decreased with increasing k_r. Thus, the contribution of the radiation mode is about 45% to 38%. At lower Rayleigh numbers, this contribution is further increased. We see that for the black body case with $\varepsilon = 1$, the influence of surface radiation is important and non-negligible. The combined Nusselt number, $Nu_t = Nu_c + Nu_r$ is an increasing function of the Rayleigh number and decreasing function of the conductivity ratio, as it should. The volume flow rate as a function of Rayleigh number with k_r as a parameter for the same case is also presented in Fig. 8. Following the results of Nu_t in the same figure, we observe that $\dot{V}$ is an increasing function of Ra and a decreasing function k_r except at low Rayleigh numbers where there is no discernible difference.

4.3. Effect of surface emissivity

The effect of the surface emissivity, ε on the heat transfer is presented as Nu_i (i stands for c, r and t) as a function of the Rayleigh number in Fig. 9 for the case of $A = 1$, $l/H = 0.05$ and $k_r = 20$ with $\varepsilon = 0$, 0.5 and 1.0. As expect, for $\varepsilon = 0$, the natural convection increases with increasing Rayleigh number and the radiation Nusselt number, Nu_r is nil. For $\varepsilon = 0.5$, the convection Nusselt number has the same trend as for $\varepsilon = 0$; however, it is slightly reduced, because of the effect of the surface radiation. The radiation Nusselt number, Nu_r is quasi-constant with Ra. For $\varepsilon = 1$, the convection Nusselt number, Nu_c has the same trend but it is further reduced with respect to that for $\varepsilon = 0.5$; the radiation Nusselt number, Nu_r is quasi-constant with Ra and increased considerably with respect to that for $\varepsilon = 0.5$, both results are also as expected. The reason for the constancy of Nu_r for $\varepsilon > 0$ with Ra is due to the fact that following Eq. (8), the radiation number N_r is a decreasing function of Ra, the radiative heat flux ς is an increasing function of Ra and the wall surface temperature θ_1 is a decreasing function of Ra. As a result, the nominator and the denominator of Eq. (8) vary almost at the same rate and Nu_r becomes quasi-constant. We note also that at $Ra = 10^{12}$ for example, the combined Nusselt number, Nu_t is increased by about 43% with $\varepsilon = 0.5$ and 66% for $\varepsilon = 1$ when compared to the case with $\varepsilon = 0$. A cross plot of the data as Nu_i versus ε for the same case showed that Nu_c is a decreasing function of the emissivity ε while the radiation Nusselt number, Nu_r is an increasing function of it. The trend of combined Nusselt number, Nu_t is controlled by the surface radiation as a consequence of which it is an increasing function of the emissivity, ε.

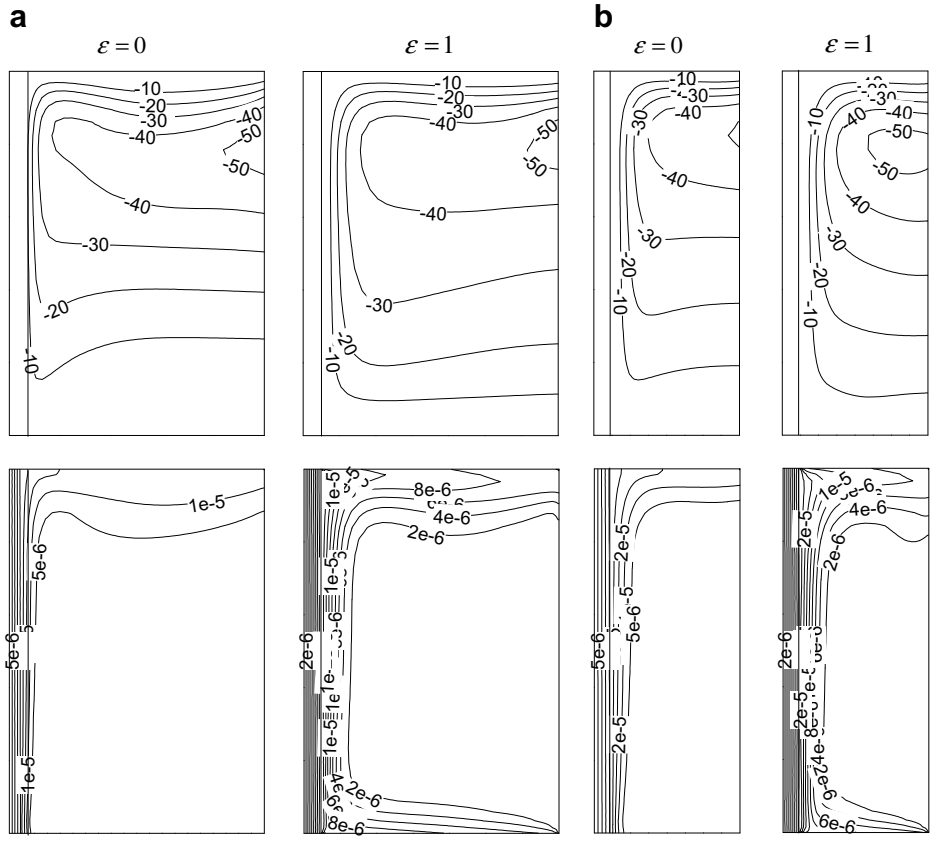

Fig. 4. Streamlines and isotherms, for $l/H = 0.05$, $\varepsilon = 0$ and 1.0, $Ra = 10^{11}$ and $k_r = 20$. (a) $A = 0.7$, (b) $A = 0.4$.

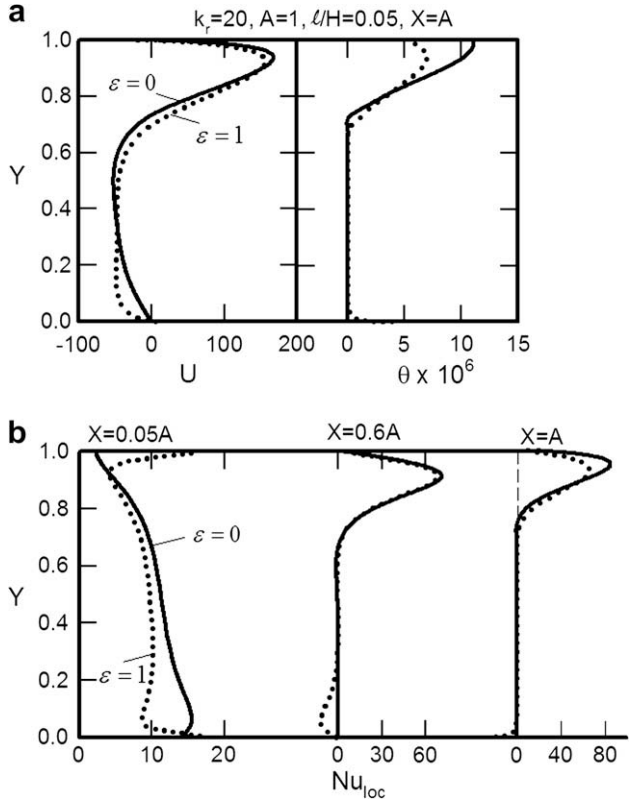

Fig. 5. For the case of $A = 1$, $l/H = 0.05$, $k_r = 20$, $\varepsilon = 0$ and 1.0, and at $Ra = 10^{10}$. (a) velocity and temperature profiles at the exit plane, (b) the convective local Nusselt number at three vertical planes.

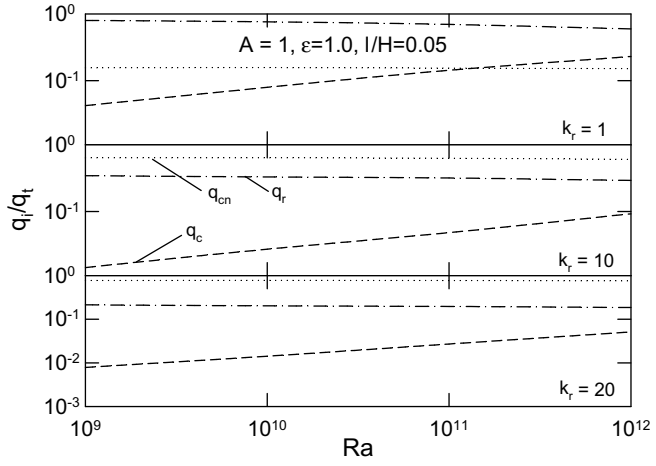

Fig. 6. Heat flux by conduction, radiation and natural convection as a function of the Rayleigh number for the case $A = 1$, $l/H = 0.05$, $k_r = 1$–20 and $\varepsilon = 1.0$.

4.4. Effect of wall thickness

This is essentially the effect of wall conductance on the heat transfer by convection and radiation. It is expected that the combined heat transfer by convection and radiation will be reduced as the conductance is increased, i.e. as the wall thickness for a given conductivity ratio is decreased. The results of Nu_i and $\dot{V}$ as a function of l/H for the case of $A = 1$ with $k_r = 20$ and for $\varepsilon = 0$ and 1.0 at $Ra = 10^{10}$ and 10^{12} are presented in Fig. 10. As we can see, for increasing wall thickness, l/H, the conductance becomes smaller as a result of which Nu_c and $\dot{V}$ are increased for both $\varepsilon = 0$

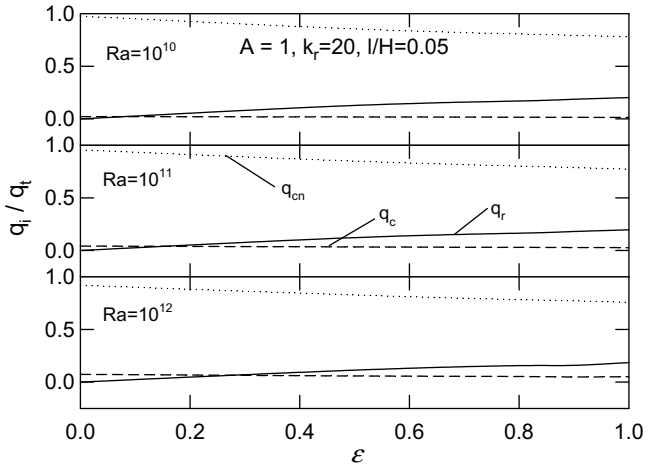

Fig. 7. Heat flux by conduction, radiation and natural convection as a function of the surface emissivity for the case $A = 1$, $l/H = 0.05$, $k_r = 20$ and $Ra = 10^{10}$, 10^{11} and 10^{12}.

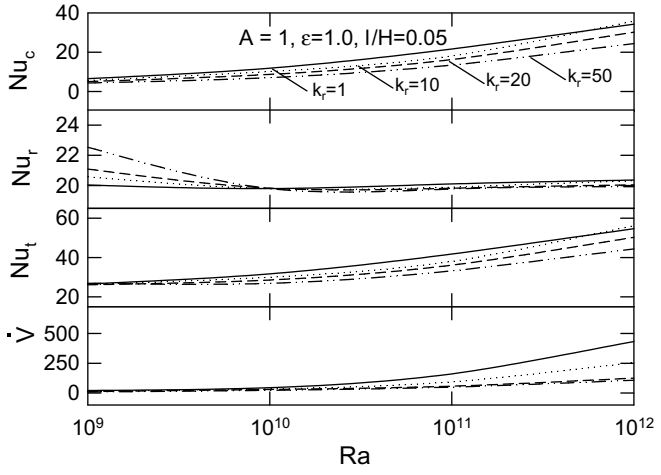

Fig. 8. Convection, radiation and combined Nusselt numbers, and the volume flow rate as a function of the Rayleigh number with k_r as a parameter presented for the case of $A = 1$, $l/H = 0.05$ and $\varepsilon = 1.0$.

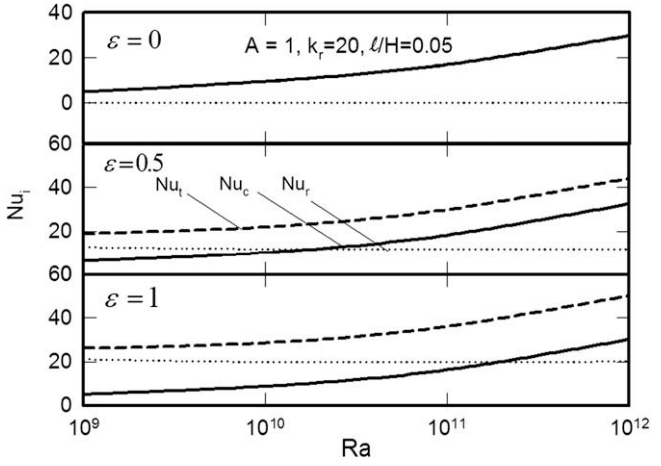

Fig. 9. Convection, radiation and combined Nusselt numbers as a function of the Rayleigh number with ε as a parameter presented for the case of $A = 1$, $l/H = 0.05$ and $k_r = 20$.

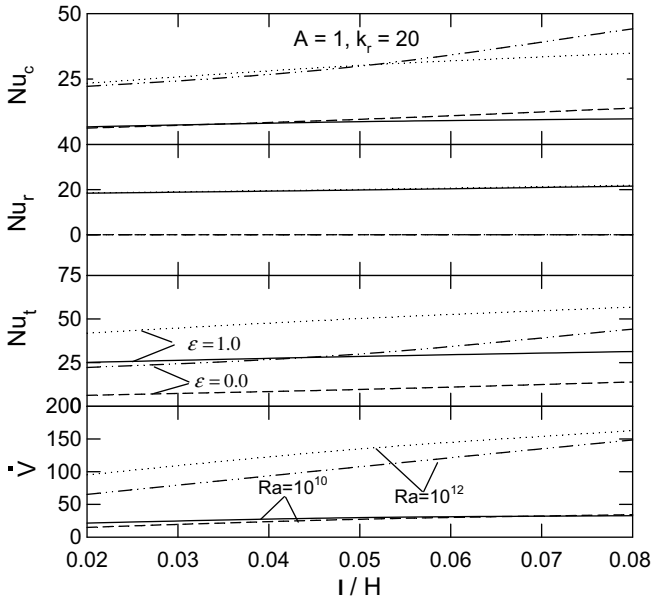

Fig. 10. Convection, radiation and combined Nusselt numbers, and the volume flow rate as a function of the wall thickness, l/H with ε and Ra as parameters presented for the case of $A = 1$ and $k_r = 20$.

and 1.0. The effect is more accentuated at higher Rayleigh numbers. Nu_r is nil for $\varepsilon = 0$ and slightly increasing function of l/H. This is expected since the surface radiation is quasi-independent of the wall thickness. The trend of Nu_t is controlled by the convective Nusselt number: generally, Nu_t and $\dot{V}$ are an increasing function of l/H.

4.5. Effect of aspect ratio

The effect of the aspect ratio, A on the heat transfer, Nu_i and volume flow rate, $\dot{V}$ is presented in Fig. 11 for the case of $l/H = 0.05$ with $k_r = 20$ and for $\varepsilon = 0$ and 1.0 at $Ra = 10^{10}$ and 10^{12}. For $\varepsilon = 0$, the radiation exchange is zero, the convection is slightly decreasing

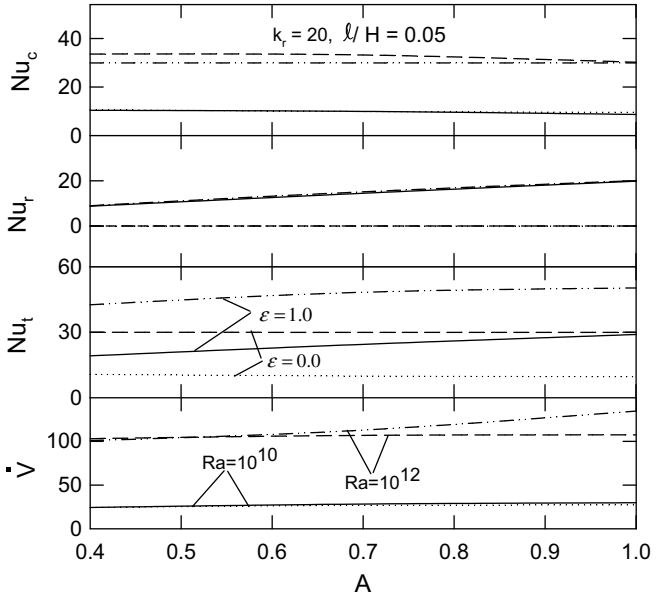

Fig. 11. Convection, radiation and combined Nusselt numbers, and the volume flow rate as a function of the aspect ratio, A with ε and Ra as parameters presented for the case of $l/H = 0.05$ and $k_r = 20$.

function of the aspect ratio for both Rayleigh numbers. This is expected since the convection is stronger in tall cavities with larger openings. For $\varepsilon = 1$, the radiation heat exchange is an increasing function of the aspect ratio, A, and the effect of the Rayleigh number is negligibly small. This is also expected since the surface radiation from relatively larger area has a bigger contribution as A is increased. For the same reason as for $\varepsilon = 0$, the heat transfer by convection is slightly decreasing function of it. As a result, the combined Nusselt number, Nu_t and the volume flow rate, $\dot{V}$ have a trend following Nu_c and Nu_r: for $\varepsilon = 0$, it is quasi-constant with A and for $\varepsilon = 1$, it is an increasing function of A. Both are more accentuated at higher Rayleigh numbers.

5. Conclusions

We investigated conjugate heat transfer by conduction, natural convection and radiation in open cavities. The heat source is applied to the vertical wall with finite thickness facing the opening. The aspect ratio was varied from 0.4 to 1 and the wall thickness from 0.02 to 0.08. The Rayleigh number varied from 10^9 to 10^{12}, the conductivity ratio from 1 to 50; the Prandtl number was 0.7. Conservation equations of mass, momentum and energy were solved by finite difference–control volume numerical method. In view of the results presented, the main points can be summarized as follows.

The surface radiation modifies the flow and temperature fields. The modification starts at low surface emissivity and increases gradually with it. The distribution of the heat flux by conduction and natural convection is affected by the surface radiation; the heat flux is an increasing function of the surface emissivity as a result of which heat fluxes by natural convection and conduction are decreased with the surface emissivity. On the other hand, the convective and radiative Nusselt numbers are both increasing functions of the surface emissivity for a given conductivity ratio and wall thickness.

The conductivity ratio and the wall thickness affect heat transfer by natural convection and by surface radiation. Heat transfer by natural convection and by surface radiation is a decreasing function of the conductivity ratio and increasing function of the wall thickness. As a result, the Nusselt numbers by natural convection and radiation are a decreasing function of the conductivity ratio and an increasing function of the wall thickness at a given surface emissivity.

The natural convection Nusselt number is a decreasing function of the aspect ratio. The radiation Nusselt number and the volume flow rate are increasing function of it.

Acknowledgement

The financial support for this study by Natural Sciences and Engineering Research Council Canada is acknowledged.

References

[1] E. Bilgen, Passive solar massive wall systems with fins attached on the heated wall and without glazing, J. Solar Energy Eng. 122 (2000) 30–34.
[2] W. Chakroun, Effect of boundary wall conditions on heat transfer for fully open tilted cavity, J. Heat Transfer 126 (2004) 915–923.
[3] P. Le Quere, J.A. Humphrey, F.S. Sherman, Numerical calculation of thermally driven two-dimensional unsteady laminar flow in cavities of rectangular cross section, Numer. Heat Transfer 4 (1981) 249–283.
[4] F. Penot, Numerical calculation of two-dimensional natural convection in isothermal open cavities, Numer. Heat Transfer 5 (1982) 421–437.
[5] Y.L. Chan, C.L. Tien, A numerical study of two-dimensional natural convection in square open cavities, Numer. Heat Transfer 8 (1985) 65–80.
[6] A.A. Mohamad, Natural convection in open cavities and slots, Numer. Heat Transfer 27 (1995) 705–716.
[7] Y.L. Chan, C.L. Tien, A numerical study of two-dimensional laminar natural convection in shallow open cavities, Int. J. Heat Mass Transfer 28 (3) (1985) 603–612.
[8] O. Polat, E. Bilgen, Laminar natural convection in shallow open cavities, Int. J. Therm. Sci. 41 (2002) 360–368.
[9] O. Polat, E. Bilgen, Conjugate heat transfer in inclined open shallow cavities, Int. J. Heat Mass Transfer 46 (2003) 1563–1573.
[10] O. Polat, E. Bilgen, Natural convection and conduction heat transfer in shallow cavities with bounding walls, Heat Mass Transfer 41 (2005) 931–939.
[11] V. Sernas, I. Kyriakides, Natural convection in an open cavity, Proc. Seven. Int. Heat Transfer Conf. Munich 2 (1982) 275–286.
[12] C.F. Hess, R.H. Henze, Experimental investigation of natural convection losses from open cavities, J. Heat Transfer 106 (1984) 333–338.
[13] S.S. Cha, K.J. Choi, An interferometric investigation of open cavity natural convection heat transfer, Exp. Heat Transfer 2 (1989) 27–40.
[14] Y.L. Chan, C.L. Tien, Laminar natural convection in shallow open cavities, J. Heat Transfer 108 (1986) 305–309.
[15] M. Akiyama, Q.P. Chong, Numerical analysis of natural convection with surface radiation in a square cavity, Numer. Heat Transfer Part a 31 (1997) 419–433.
[16] N. Ramesh, S.P. Venkateshan, Effect of surface radiation on natural convection in a square enclosure, J. Thermophys. Heat Transfer 13 (3) (1999) 299–301.
[17] N. Ramesh, W. Merzkirch, Combined convective and radiative heat transfer in side-vented open cavities, Int. J. Heat Fluid Flow 22 (2) (2001) 180–187.
[18] S.N. Singh, S.P. Venkateshan, Numerical study of natural convection with surface radiation in side-vented open cavities, Int. J. Therm. Sci. 43 (9) (2004) 865–876.
[19] A.A. Dehghan, M. Behnia, Combined natural convection–conduction and radiation in a discretly heated open cavity, J. Heat Transfer 118 (1996) 56–64.
[20] J.F. Hinojosa, R.E. Cabannilas, G. Alvarez, C.E. Estrada, Nusselt number for the natural convection and surface thermal radiation in a square tilted open cavity, Int. Commun. Heat Mass Transfer 32 (2005) 1184–1192.
[21] R. Siegel, J.R. Howell, Thermal Radiation Heat Transfer, second ed., Hemisphere Publishing Corporation, Washington, 1981.
[22] S.V. Patankar, Numerical Heat Transfer and Fluid Flow, Hemisphere Publishing Corporation, New York, 1980.
[23] D. de Vahl Davis, Natural convection of air in a square cavity: a benchmark solution, Int. J. Num. Methods Fluids 3 (1983) 249–264.